ration to dryness, was submitted to TLC in chloroform giving (decreasing R_fs) diradical •PTM-PTM• (0.056 g, 28% recovery), fuchsone radical III (0.08 g, 41% yield), and difuchsone II (0.044 g, 23%). III: orange-red solid; mp 316-319 °C dec; UV-vis ($CHCl_3$) (supplementary material, Figure 6) 285 nm, 365 (sh), 385, 420, 560 (ϵ 15 500, 29 400, 53 300, 23 000, 1240); IR (KBr) 1660, 1650, 1550, 1500, 1350, 1330, 1290, 1255, 1220, 1125, 1105, 1015, 875, 865, 835, 812, 765, 755, 730, 700, 675, 650, 620-600, 535, 530, 508 cm^{-1}. ESR data: Table I. Magnetic susceptibility $X_{dia} = -0.488 \times 10^{-6}$ emu;[32] $J = -4.7$ K, $\mu = 1.71$, spin/mol = 5.92×10^{23}. Anal. Calcd for $C_{38}Cl_{27}O$: C, 31.9; H, 0.0. Found: C, 32.2; H, 0.0.

Conversion of Fuchsone Radical III into Difuchsone II. A solution of $SbCl_5$ (0.24 g, 1.1×10^{-3} mol) in CH_2Cl_2 (25 mL) was saturated with Cl_2 at room temperature, and next fuchsone radical III (0.045 g, 3.1×10^{-5} mol) was added. After stirring (24 h), water (5 mL) was added, and the CH_2Cl_2 layer was washed with aqueous HCl and dried. The solid residue (0.046 g), obtained by evaporation to dryness, was submitted to column chromatography in CCl_4, giving difuchsone II (0.043 g, 97% yield), which was identified by comparative TLC and IR.

(32) Calculated independently from modified Pascal's data.[33]
(33) Foex, G.; Goreter, C.; Smith, L. J. *Constants Selectionées. Diamagnetisme et Paramagnetisme. Relaxation Paramagnêtique*; Masson et Cie.: Paris, 1957, pp 222-225. Ballester, M.; Castañer, J.; Riera, J.; Ibáñez, A.; Pujadas, J. *J. Org. Chem.* **1982**, *47*, 259.

Acknowledgment. Thanks are due to Drs. E. Wasserman, J. S. Miller, and P. Krusic, E. I. DuPont de Nemours (Wilmington, DE) for providing us with complementary ESR data, to Mrs. A. Díez for the ESR measurements, and to Mr. J. Vidal for his experimental assistance. I.P. wishes to express her gratitude to the Spanish Ministry of Education and Science for a doctoral fellowship during the period 1985-1989.

Supplementary Material Available: UV-vis spectra of cations (Figure 5) and of fuchsone I and difuchsone II (2 pages). Ordering information is given on any current masthead page.

Macrocyclic Trinucleating Ligands for the Cocomplexation of Two "Soft" (Cu^{2+}, Ni^{2+}, or Zn^{2+}) Metal Centers and One "Hard" (Ba^{2+} or Cs^{+}) Metal Center[1]

Frank C. J. M. van Veggel,[†] Martinus Bos,[‡] Sybolt Harkema,[§] Henry van de Bovenkamp,[†] Willem Verboom,[†] Jan Reedijk,[⊥] and David N. Reinhoudt*[,†]

Laboratories of Organic Chemistry, Chemical Analysis, and Chemical Physics, University of Twente, P.O. Box 217, 7500 AE Enschede, The Netherlands, and Department of Chemistry, Gorlaeus Laboratories, Leiden University, 2300 RA Leiden, The Netherlands

Received June 27, 1990

Macrocyclic heterotrinucleating ligands that have one compartment for complexation of alkaline or alkaline earth cations and two compartments for transition-metal cations have been synthesized. The Ba^{2+}-templated (2 + 2) macrocyclization of the dialdehydes **3a** and **3b** with the diamine **8** yielded the barium complexes (**9b**, **9e**) in high yield. The Cs^{+}-templated (2 + 2) macrocyclization of the dialdehyde **3a** and the diamine **8** gave the cesium complex **9c**. The mononuclear complexes were converted into the heterotrinuclear complexes **10a-h** by reaction with 2 equiv of copper, nickel, or zinc acetate. The barium complex **9b**, the dicopper/barium complex **10a**, and the dinickel/barium complex **10b** have been analyzed by X-ray crystallography. In all three crystal structures the O_{10} cavity is folded around the barium cation. The copper-copper distance in the dicopper/barium complex **10a** is 3.50 Å and the nickel-nickel distance in the dinickel/barium complex **10b** is 3.42 Å. The electrochemistry of the copper-containing heterotrinuclear complexes **10a**, **10d**, and **10g** and the nickel-containing heterotrinuclear complexes **10b**, **10e**, and **10h** has been studied by polarography, cyclic voltammetry, and coulometry in DMSO. The dinickel/barium complex **10b** was also studied by Kalousek polarography. The dicopper/metal complexes **10a**, **10d**, and **10g** all show a copper-copper interaction, which is the strongest for the dicopper/barium complex **10a**. Coulometry revealed that the complexes **10a**, **10d**, and **10g** undergo a reduction with two electrons, and cyclic voltammetry showed that the reduction/oxidation processes of **10a**, **10d**, and **10g** are chemically reversible. The reduction/oxidation processes of the nickel-containing heterotrinuclear complexes **10b**, **10e**, and **10h** are complicated by adsorption phenomena. Frozen EPR spectra of **10a** and **10g** exhibit typical triplet spectra with a zero-field splitting of about 0.04 cm^{-1}. This behavior is typical for Cu(II) dimers and confirms that both Cu(II) cations are also exchange coupled in solution. A Cu-Cu distance in solution of 3.6 Å agrees best with the spectra. Attempts to add exogenous bridging ligands like F^{-} and imidazolate were unsuccessful.

Introduction

The dicopper metalloproteins hemocyanine and tyrosinase contain two Cu(I) metal cations in the active site.[2] The crystal structure of the deoxy state of hemocyanine has been recently published.[3] The two Cu(I) cations are both coordinated by three nitrogen atoms from histidines and the intermetallic distance is about 3.5 Å without a bridging anion. The active site of tyrosinase is similar to that of hemocyanine.[2]

[†] Laboratory of Organic Chemistry, University of Twente.
[‡] Laboratory of Chemical Analysis, University of Twente.
[§] Laboratory of Chemical Physics, University of Twente.
[⊥] Department of Chemistry, Leiden University.

(1) Part of this work has appeared as a preliminary communication: van Veggel, F. C. J. M.; Bos, M.; Harkema, S.; Verboom, W.; Reinhoudt, D. N. *Angew. Chem., Int. Ed. Engl.* **1989**, *28*, 746.
(2) See for recent reviews of dicopper metalloproteins and synthetic analogues: (a) Latour, J.-M. *Bull. Soc. Chim. Fr.* **1988**, 508. (b) Sorrell, T. N. *Tetrahedron* **1989**, *45*, 3.
(3) (a) Linzen, B.; Soeter, N. M.; Riggs, A. F.; Schneider, H.-J.; Schartau, W.; Moore, M. D.; Yokota, E.; Behrens, P. Q.; Nakashima, H.; Takagi, T.; Nemoto, J. M.; Verijken, J. M.; Bak, H. B.; Beintena, J. J.; Volbeda, A.; Gaykema, W. P. J.; Hol, W. G. J. *Science (Washington D.C.)* **1985**, *229*, 519. (b) Volbeda, A.; Hol, W. G. J. *J. Mol. Biol.* **1989**, *209*, 249.

0022-3263/91/1956-0225$02.50/0

Dinuclear copper complexes without a bridging ligand are interesting as models for copper proteins.[4] Many synthetic models have been published in order to mimic the active site.[2] However, almost all reported synthetic analogues that should mimic the active site contain dinucleating ligands in which a hydroxide, a phenolate, or an alkoxide group acts as an exogenous or endogenous bridge between the two copper sites. The bridging anion brings and maintains the two copper cations in close proximity (Cu···Cu < 4.5 Å).

The number of dinuclear complexes without a bridging anion and a short intermetallic distance is limited; some of them will be briefly mentioned. The dinickel(II) complex of a 28-membered ring with eight sulfur donor atoms has been reported by Travis and Busch.[5] The metal to metal distance was not reported, but the physical measurements indicate that the octadentate ligand gives a complex in which the two nickel cations are each coordinated to four donor atoms.

The crystal structure of the dicopper(II) complex of an octaaza-crown ether has been reported by Mertes.[6] The two copper ions are arranged cofacially at a distance of 5.39 Å. Another way of positioning two transition-metal cations without a bridging anion is possible in macrotricyclic ligands. Lehn[7] and Weiss[8] have reported dinuclear Cu(II) complexes of these ligands with an intermetallic distance larger than 5 Å. Maverick[9] has investigated a number of cofacial dinuclear bis(β-keto enamine) complexes. With xylyl groups as spacers they observed metal to metal distances of 4.3–4.4 Å for dinickel, dicopper, and dipalladium complexes.

Both Karlin[10] and Kitajima et al.[11] have reported the crystal structure of a dinuclear copper complex in which dioxygen (O_2) is bound. In both cases the dinuclear complex is obtained by reaction of two Cu(I) complexes with O_2. In the structure published by Karlin, the peroxide is complexed in a μ-1,2-fashion, whereas in the complex published by Kitajima et al. the peroxide is bound in a μ-η^2-η^2-fashion.

Previously, we[12] have published a dicopper(I) complex of an acyclic ligand with four benzimidazole groups, in which both copper ions are coordinated by two nitrogens of two benzimidazole groups in an almost linear fashion. The observed Cu···Cu distance was 3.04 Å. Short metal-to-metal distances can also be achieved in monocyclic ligands. Gould et al.[13] have found a Cu···Cu distance of 4.25 Å in the dicopper(I) complex of hexathia-18-crown-6.

As part of our investigations on the complexation of polar neutral guests in macrocyclic compounds we have shown that "immobilized" cations, chelated in salen type ligands, can assist in the complexation by coordination of the guest to a vacant site.[14] Heterodinuclear complexes can be easily obtained by cocomplexation of "hard" cations, like alkaline and alkaline earth cations, in the crown ether cavities of these macrocyclic ligands with immobilized transition-metal cations.[15] X-ray analysis of a number of heterodinuclear complexes[15] showed that the intermetallic distance of 3.63–3.73 Å is hardly sensitive to the structural changes of the ditopic ligands, possibly due to the bridging phenolate anions. Electrochemistry revealed that upon cocomplexation of hard cations in the crown ether cavities in general anodic shifts of the reduction potential are observed.

Based on our simple methodology we like to report in this paper a *novel* way to organise two soft metal cations at short distances in macrocyclic ligands by cocomplexation of a hard alkaline or alkaline earth cation. The synthesis, X-ray structures, electrochemistry, and EPR properties of the heterotrinuclear complexes will be discussed.

Scheme I

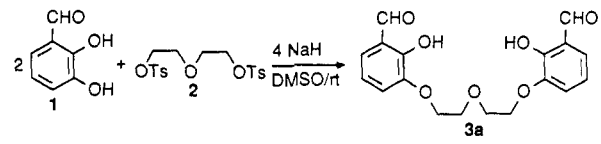

Scheme II

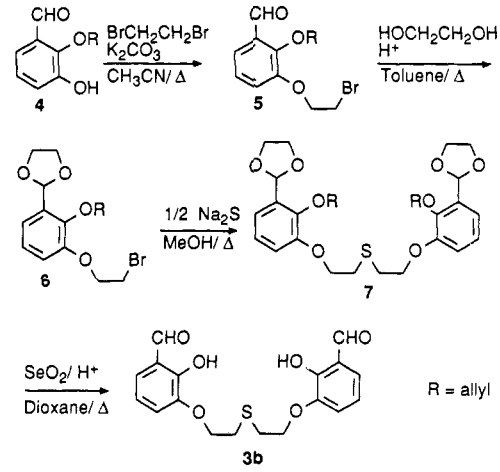

Results and Discussion

Synthesis. The dialdehyde **3a** (Scheme I) was prepared in 49% yield by reaction of the dianion of **1**[16] with diethylene glycol ditosylate (**2**) in DMSO, followed by acidic workup and chromatography. A different route (Scheme II) was followed for the synthesis of the dialdehyde **3b**, because the ditosylate of diethanol sulfide is a mustard equivalent, and therefore we decided to avoid this compound. The 2-hydroxyl group of 2,3-dihydroxybenzaldehyde (**1**) was protected by reaction with allyl bromide to give **4**.[14] Subsequent reaction with excess of 1,2-dibromoethane in refluxing acetonitrile with K_2CO_3 as a base gave **5** in a yield of 98%. The aldehyde functionality was protected as a cyclic acetal by reaction with ethylene glycol

(4) (a) Ghosh, P.; Tyeklar, Z.; Karlin, K. D.; Jacobson, R. R.; Zubieta, J. *J. Am. Chem. Soc.* **1987**, *109*, 6889. (b) Casella, L.; Gullotti, M.; Pallanza, G.; Rigoni, L. *J. Am. Chem. Soc.* **1988**, *110*, 4221. (c) Tyeklar, Z.; Karlin, K. D. *Acc. Chem. Res.* **1989**, *22*, 241.

(5) Travis, K.; Busch, D. H. *J. Chem. Soc., Chem. Commun.* **1970**, 1041.

(6) Acholla, F. V.; Takusagawa, F.; Mertes, K. B. *J. Am. Chem. Soc.* **1985**, *107*, 6902.

(7) (a) Lehn, J.-M. *Pure Appl. Chem.* **1980**, *52*, 2441. (b) Lehn, J.-M.; Simon, J. *Helv. Chim. Acta* **1977**, *60*, 141.

(8) Louis, R.; Agnus, Y.; Weiss, R. *J. Am. Chem. Soc.* **1978**, *100*, 3604.

(9) Bradbury, J. R.; Hampton, J. L.; Martone, D. P.; Maverick, A. W. *Inorg. Chem.* **1989**, *28*, 2392.

(10) Jacobson, R. R.; Teyklar, Z.; Farooq, A.; Karlin, K. D.; Liu, S.; Zubieta, J. *J. Am. Chem. Soc.* **1988**, *110*, 3690.

(11) Kitajima, N.; Fujisawa, K.; Moro-oka, Y. *J. Am. Chem. Soc.* **1989**, *111*, 8975.

(12) Hendriks, H. M. J.; Birker, P. J. M. W. L.; van Rijn, J.; Verschoor, G. C.; Reedijk, J. *J. Am. Chem. Soc.* **1982**, *104*, 3607.

(13) Gould, R. O.; Lavery, A. J.; Schröder, M. *J. Chem. Soc., Chem. Commun.* **1985**, 1492.

(14) van Staveren, C. J.; van Eerden, J.; van Veggel, F. C. J. M.; Harkema, S.; Reinhoudt, D. N. *J. Am. Chem. Soc.* **1988**, *110*, 4994.

(15) (a) van Veggel, F. C. J. M.; Harkema, S.; Bos, M.; Verboom, W.; van Staveren, C. J.; Gerritsma, G. J.; Reinhoudt, D. N. *Inorg. Chem.* **1989**, *28*, 1133. (b) van Veggel, F. C. J. M.; Harkema, S.; Bos, M.; Verboom, W.; Klein Woolthuis, G.; Reinhoudt, D. N. *J. Org. Chem.* **1989**, *54*, 2351.

(16) Kessar, S. V.; Gupta, Y. P.; Mohammed, T.; Goyal, M.; Sawal, K. K. *J. Chem. Soc., Chem. Commun.* **1983**, 400.

Scheme III

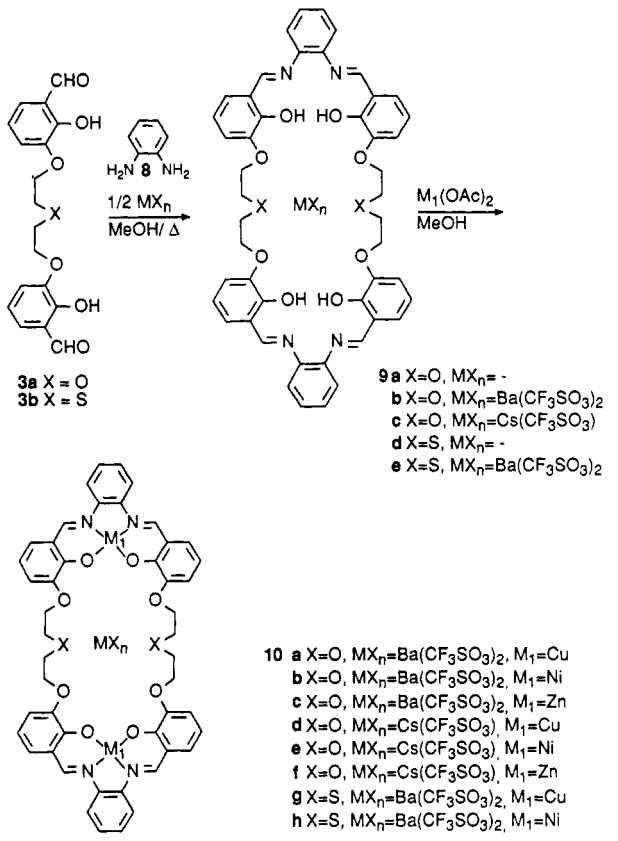

and a catalytic amount of acid in refluxing toluene to give **6** in 98% yield. The bromide **6** was converted into the sulfide **7** by reacting with 0.5 equiv of Na_2S in refluxing MeOH (yield 84%). Known procedures to remove an allyl group like reactions with K-O-*t*-Bu,[17] $Na(CH_3OCH_2CH_2O)_2AlH_2$,[18] and $Pd(OAc)_2/Ph_3P/Et_3N/HCOOH$[19] failed. However, deprotection of the allyl group was finally achieved by treatment with SeO_2 and AcOH in refluxing dioxane.[20] Acidic workup and chromatography gave the dialdehyde **3b** in a low yield of 16%.

The (2 + 2) macrocyclization of the dialdehyde **3a** and *o*-phenylenediamine (**8**) was carried out by the simultaneous slow addition of a solution of **3a** and a solution of **8** to a refluxing solution of $Ba(CF_3SO_3)_2$ or $Cs(CF_3SO_3)$ in MeOH (Scheme III). The complexes **9b** (63%) and **9c** (69%) were obtained as orange red and orange crystalline materials, respectively. The parent peaks in the FAB mass spectra of **9b** (*m/e* 1132) and of **9c** (*m/e* 970) correspond to $[M - CF_3SO_3]^+$ and $[M - CF_3SO_3 + H]^+$, respectively. The ^1H NMR spectra show the imine protons at δ 8.92 ppm (**9b**) and δ 8.80 ppm (**9c**), and in the IR spectra the stretching frequency of the imine double bonds is present at 1620 cm^{-1} (**9b**) and 1613 cm^{-1} (**9c**). The ^1H NMR spectra of **9b** and **9c** exhibit the absorption of the phenolic hydrogens at low field, δ 13.37 and 13.50 ppm, respectively, which shows that they are very acidic. One hydrogen in a salophen unit will most likely be bound to the phenolic oxygen atom and hydrogen bonded to the imine nitrogen atom, whereas the other hydrogen will most likely be bound to the imine nitrogen atom and hydrogen bonded to the phenolate oxygen atom. This has been observed in the crystal structure of a related barium complex.[14]

Table I. Selected Distances (Å) and Angles (deg) and Coordination Number

	9b			
	$Ba(1)^{2+}$	$Ba(2)^{2+}$	**10a**·$2H_2O$	**10b**·(H_2O, DMSO)
$Ba\cdots O_{phenol(ate)}$	2.69–2.97	2.70–2.91	2.75–3.10	2.72–2.85
$Ba\cdots O_{ether}$	2.80–3.14	2.82–3.20	2.82–3.11[f]	2.81–3.09
$M_1\cdots O_{phenolate}$			1.90–1.92	1.83–1.87
$M_1\cdots N$			1.88–1.98	1.84–1.86
$Ba\cdots M_1$			3.70, 3.85	3.66, 3.73
$M_1\cdots M_1$			3.50	3.42
coord no. of Ba^{2+}	11[d]	11[e]	11[g]	11[h]
∠Ar $rings_{opp}$[a]	29.5	15.6	8.2	6.5
	17.3	13.3	8.7	13.8
∠Ar $rings_{adj}$[b]	4.8/26.4	7.2/8.4	4.9/7.8	3.1/9.6
	11.2/28.2	9.3/22.7	6.5/8.5	3.8/13.0
∠N_2O_2-planes[c]	12.6	10.5	5.8	7.4

[a] Angle between the opposite aromatic rings in one salophen moiety. [b] Angles between adjacent aromatic rings in one salophen moiety. [c] Angle between the mean planes through the hetero-atoms of the salophen moiety. [d] +1 $CF_3SO_3^-$ (Ba···O 2.82 Å). [e] +1 $CF_3SO_3^-$ (Ba···O 2.82 Å). [f] +a weak coordination of a Ar–O–CH_2 oxygen atom (Ba···O 3.63 Å). [g] +1 $CF_3SO_3^-$ (Ba···O 2.89 Å) and 1 water molecule (Ba···O 3.01 Å). [h] +1 water molecule (Ba···O 2.87 Å).

The cyclization of the dialdehyde **3b** and the diamine **8** could not be effected using $Cs(CF_3SO_3)$ as template salt, but $Ba(CF_3SO_3)_2$ again proved a suitable template salt (Scheme III). The barium complex **9e** was obtained as an orange crystalline material. The FAB mass spectrum exhibits the highest *m/e* peak at 1155, which is in agreement with the calculated value for $[M - CF_3SO_3]^+$. A singlet in the ^1H NMR spectrum for the imine protons was observed at δ 8.94 ppm and the adsorption for the phenolic hydrogens is located at δ 13.29 ppm. The same accounts for this as for the compounds **9b** and **9c**. The imine double bonds show an absorption in the IR spectrum at 1621 cm^{-1}.

The complexes **9** could easily be converted into the heterotrinuclear complexes **10** by reaction with 2 equiv of copper, nickel, and zinc acetate in MeOH.[21] All the complexes **10** show in the FAB mass spectra the highest *m/e* peak that corresponds to the calculated value of $[M - CF_3SO_3]^+$. The IR spectra of **10** show the imine double bonds at lower values (1608–1610 cm^{-1}) with respect to the Ba^{2+} and Cs^+ complexes **9**, except for **10f** (1614 and 1613 cm^{-1}, respectively). Except for the dizinc/cesium complex **10f** the signals of the imine protons in the ^1H NMR spectra are shifted upfield with respect to the mononuclear Ba^{2+} and Cs^+ complexes **9**.

X-ray Structures. The solid-state structures of the compounds **9b**, **10a**·$2H_2O$, and **10b**·(H_2O, DMSO) were determined by X-ray crystallography. Details of the structure determination are given in the Experimental Section. ORTEP[22] views of the structures of **9b**, **10a**, and **10b** are shown in the Figure 1, parts a–c, respectively. Metal coordination is depicted by open bonds. Table I contains selected distances and angles and the coordination number of Ba^{2+}. Table II contains the crystal data and data collection parameters.

Ruby red crystals of the barium complex **9b** were obtained by slow diffusion of petroleum ether into a solution of **9b** in MeOH. The asymmetric unit contains two in-

(17) Gigg, J.; Gigg, R. *J. Chem. Soc. C* **1966**, 82.
(18) Kametani, T.; Huang, S. P.; Ihara, M.; Fukumoto, K. *J. Org. Chem.* **1976**, *41*, 2545.
(19) Yamada, T.; Goto, K.; Mitsuda, Y.; Tsuji, J. *Tetrahedron Lett.* **1987**, *28*, 4557.
(20) Kariyone, K.; Yazawa, H. *Tetrahedron Lett.* **1970**, 2885.
(21) The barium free dicopper and dinickel complexes could be made by reaction of **9a** with two equiv of copper(II) and nickel(II) acetate, respectively, but these complexes are insoluble in all normal organic solvents.
(22) Johnson, C. K.; ORTEP, Report ORNL-3794; Oak Ridge National Laboratory, Oak Ridge, TN, 1965.

Table II. Crystal Data and Data Collection Parameters

	9b	10a·2H$_2$O	10b·(H$_2$O, DMSO)
formula	$C_{50}H_{44}BaF_6N_4O_{16}S_2$	$C_{50}H_{44}BaCu_2F_6N_4O_{18}S_2$	$C_{52}H_{48}BaF_6N_4Ni_2O_{18}S_3$
fw	1272.35	1431.43	1481.86
lattice type	triclinic	orthorhombic	triclinic
space group	$P\bar{1}$	*Pbca*	$P\bar{1}$
T, K	293	293	293
cell dimensions			
a, Å	21.950 (2)	28.589 (9)	14.280 (6)
b, Å	16.993 (2)	27.786 (4)	15.209 (7)
c, Å	14.503 (2)	13.383 (3)	15.823 (2)
α, deg	84.15 (5)		67.86 (2)
β, deg	79.04 (5)		71.16 (2)
γ, deg	88.79 (5)		60.62 (3)
V, Å^3	5283 (8)	10631 (6)	2733 (3)
Z	4	8	2
D_c, g cm^{-3}	1.60	1.74	1.53
$F(000)$	2568	5728	1492
μ, cm^{-1}	9.2	16.9	15.5
θ range, deg	3–25	3–22.5	3–25
no. of unique reflns			
measd	4459	6904	9607
obsd[a]	4388	2586	7079
no. of variables	387	356	518
R, %	6.0	7.8	6.1
R_w, %	6.8	9.0	8.2
weighting factor p	0.04	0.05	0.04
extinction g ($\times 10^{-7}$)	–	–	0.69

[a] $I > 5\sigma(I)$ for **9b** and **10a**·2H$_2$O and $I > 3\sigma(I)$ for **10b**·(H$_2$O, DMSO).

dependent molecules of which one is shown in Figure 1a.

The barium cation in molecule 1 (Figure 1a) is surrounded by the 10 oxygens of the macrocyclic ring (Ba···O 2.69–3.14 Å) and one oxygen of a coordinated triflate anion (Ba···O 2.82 Å). The two conjugated systems show a large deviation from planarity (the angles between the two opposite aromatic rings are 29.5° and 17.3°). The mean planes through the heteroatoms of the salophen unit are nearly parallel, with an angle of 12.6°.

The conformation of molecule 2 resembles that of molecule 1. The barium is also 11-fold coordinated by the 10 oxygens of the macrocyclic ring (Ba···O 2.70–3.20 Å) and one oxygen of a triflate anion (Ba···O 2.82 Å). The deviation from planarity in the conjugated systems is somewhat smaller than in molecule 1 (the angle between the two opposite aromatic rings are 15.6° and 13.3° vs 29.5° and 17.3° for molecule 1). The mean planes through the heteroatoms of the salophen unit are nearly parallel, with an angle of 10.5°.

Suitable crystals for an X-ray analysis of the dicopper/barium complex **10a**·2H$_2$O (Figure 1b) were obtained by slow diffusion of Et$_2$O into a solution of **10a** in a mixture of MeOH and CH$_3$CN (1:1).[1] The structure is similar to that of the barium complex **9b** and to the dinickel/barium complex **10b** (vide infra). The two copper cations are complexed in a square-planar fashion in the salophen units with normal Cu···O (1.90–1.92 Å) and Cu···N (1.88–1.98 Å) distances. They are within 0.05 Å of the mean plane through the four coordinating atoms. The barium cation is complexed in the polyether cavity by nine oxygen atoms of the macrocyclic ring (Ba···O 2.76–3.11 Å) and a weak coordination of the remaining ArOCH$_2$ oxygen atom (Ba···O 3.63 Å). In addition to these 10 oxygen atoms of the macrocycle also a triflate anion (Ba···O 2.89 Å) and a water molecule (Ba···O 3.01 Å) are coordinated. The

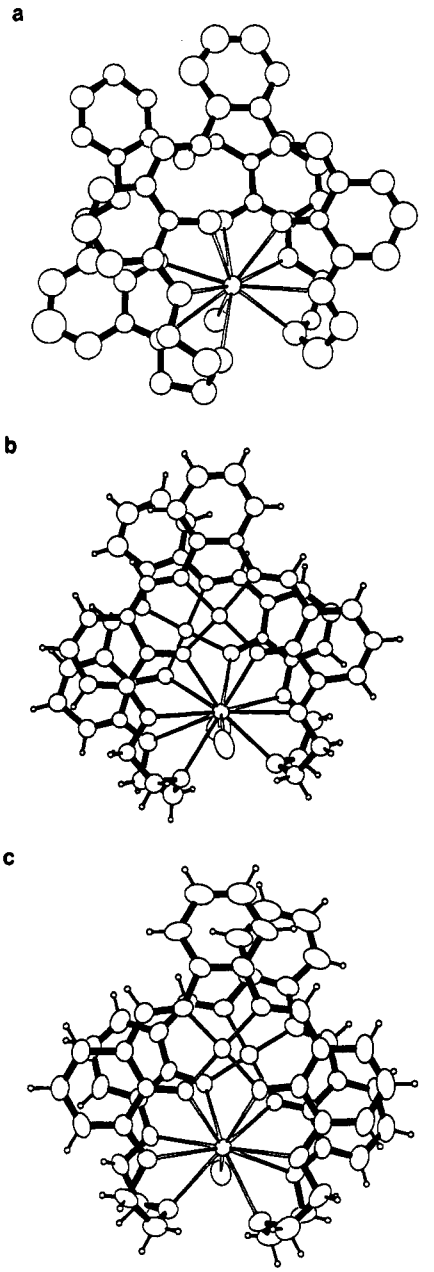

Figure 1. (a) View of **9b** (molecule 1). Only the oxygen of the coordinated anion is shown. (b) View of **10a**·2H$_2$O. Only the oxygen of the coordinated anion and water are shown. (c) View of **10b**·(H$_2$O,DMSO). Only the oxygen of the coordinated water is shown.

conjugated systems show a much smaller deviation from planarity than in the barium complex **9b** (the angle between the opposite aromatic rings in **10a** are 8.2° and 8.7°). The mean planes through the coordinating atoms of the copper ions are approximately parallel, with an angle of 5.8°. The separation of the planes is about 3.45 Å. A view perpendicular to one salophen unit shows that the other unit is not exactly under it but is displaced by about 1.4 Å. The metal–metal distances in this complex are Ba^{2+}···Cu^{2+}, 3.70 and 3.85 Å; Cu^{2+}···Cu^{2+}, 3.50 Å. The angle Cu^{2+}–Ba^{2+}–Cu^{2+} is 55.1°.

Dark red single crystals of the dinickel/barium complex **10b** were similarly obtained by slow diffusion of Et$_2$O into a solution of **10b** in a mixture of CH$_3$CN and dimethyl sulfoxide (DMSO). The structure of **10b**·(H$_2$O, DMSO) is shown in Figure 1c. The nickel cations are complexed in the salophen unit in a square-planar fashion with normal Ni···O (1.83–1.87 Å) and Ni···N (1.84–1.86 Å) distances.

Table III. Polarographic Data for the Reduction at a Dropping Mercury Electrode at 20 °C in 0.1 M TEAP in DMSO vs Ag/AgCl

compd	$E_{1/2}$, V	il, μA	slope log plot, mV	conc, mM
10a	-1.053	1.11	52	1.45
	-1.098	1.11	50	
10b	-1.036	0.60	50	1.20
	-1.137	0.70	46	
10d	-1.141	0.98	82	0.70
10e	-1.300	1.08	61	0.81
10g	-1.055	0.68	110	0.68
10h	-0.995	0.34	52	0.51
	-1.162	0.41	51	
	-1.329	0.36	65	

They are within 0.01 Å of the mean plane of the four coordinating atoms. The barium cation has an 11-fold coordination. In addition to the 10 oxygens of the macrocyclic ring (Ba···O 2.27–3.09 Å) a water molecule is coordinated (Ba···O 2.87 Å). The salophen units are not completely planar (the angles between the opposite aromatic rings in one unit are 6.5° and 13.8°). The mean planes through the coordinating atoms of the nickel ions are also approximately parallel, with an angle of 7.4°. A view perpendicular to one salophen unit shows that the other unit is not exactly under it but is displaced by about 0.95 Å. The metal–metal distances in this complex are Ba^{2+}···Ni^{2+} 3.66 and 3.73 Å; Ni^{2+}···Ni^{2+} 3.42 Å. The angle Ni^{2+}–Ba^{2+}–Ni^{2+} is 55.1°.

The striking result in the three discussed structures is that by the complete surrounding of the barium cation the two salophen units are brought into close proximity in a parallel stacking orientation. This complete surrounding of the barium cation by large macrocyclic polyether cavities has been observed before.[14,15a,23] The coordination sphere of the barium cation is often completed by anions and/or solvent molecules. By complexation of copper and nickel cations in the salophen unit a higher planarity of the conjugated system is obtained. We have found this before for the barium and nickel/barium complexes.[14,15a]

Electrochemistry. The reduction properties of the dicopper/metal complexes **10a**, **10d**, and **10g** and the dinickel/metal complexes **10b**, **10e**, and **10h** were investigated by sampled DC_T-polarography in DMSO with TEAP ($Et_4N^+ClO_4^-$) as supporting electrolyte. The DC_T-polarograms in the range of −0.2 to −1.6 V were recorded and evaluated by a computerized method described by Zollinger et al.[24] and are given in Table III. These complexes were also studied with cyclic voltammetry and coulometry, in DMSO with TEAP as supporting electrolyte. For the dinickel/barium complex **10b** also Kalousek measurements were performed, in DMSO with TEAP as supporting electrolyte. Potentials are reported vs. an Ag/AgCl reference electrode.

The DC_T polarogram of the dicopper/barium complex **10a** shows two waves with half-wave potentials ($E_{1/2}$) of −1.065 and −1.110 V, respectively.[25] The ratio of the limiting currents is 1, which is in agreement with two one-electron reductions. This was confirmed by coulometry at −1.4 V. The current–time curve shows an exponential shape and after the exchange of two electrons the current is at the background level. The cyclic voltammograms were recorded at scan rates of 0.5–6 V/s. At these scan rates the two-step process is reflected as a shoulder on the peak in the reductive as well as in the oxidative sweep. The cathodic and anodic peaks are found at −1.12 and −1.01 V, respectively, but these peaks have no physical meaning. This two-electron reduction/oxidation is *chemically reversible*, because when five scans at scan rates of 0.5 and 6 V/s were applied, five identical cyclic voltammograms were recorded. This reduction can be regarded as taking place via a simple EE-mechanism, that is, two one-electron transfers via a (formally) M_1^{II}/M_1^{I} oxidation state to a (formally) M_1^{I}/M_1^{I} oxidation state. In other words: the two copper cations interact with each other.

The DC_T polarograms of the dicopper/cesium complex **10d** and the dicopper/barium complex **10g** show one asymmetrical wave with $E_{1/2}$ of −1.141 and −1.055 V, respectively. Because of the asymmetry of the waves, the curve fitting is not very good and this may cause the relatively high slopes. The reduction of the dicopper/cesium complex **10d** takes place at a more cathodic potential compared to the reduction of the dicopper/barium complex **10a**. This can be explained by the monovalency of Cs^+ whereas Ba^{2+} is a divalent cation. We have shown that monovalent cations induce a smaller anodic shift of the reduction potential than bivalent cations.[15a] Another effect is the larger radius of Cs^+ (1.67 Å) compared to Ba^{2+} (1.34 Å), which will also reduce the electron-withdrawing ability of electrons from the salenophen unit. The more anodic reduction potential of the dicopper/barium complex **10g** may be a combination of both a smaller electron donation of the sulfur atoms toward the Ba^{2+} which will make the Ba^{2+} a stronger electrophile, and a different conformation due to different CH_2SCH_2 angles and different C–S bond distances.[26] Coulometry of both complexes at −1.4 V was performed. In both cases the current–time curves show nice exponential shapes, and the number of electrons transferred is two. The cyclic voltammograms at scan rates of 1–6 V/s were recorded, and they show one reduction and one oxidation peak between −0.2 and −1.4 V. However, the shape of the peaks is broadened with respect to "normal" cyclic voltammograms. From both the DC_T polarograms and the cyclic voltammograms it is tentatively concluded that there is an interaction between the two copper cations in **10d** and **10g**, but it is less pronounced than for **10a**.

The dinickel/metal complexes **10b**, **10e**, and **10h** showed a more complicated electrochemical behavior. The DC_T polarogram of the dinickel/barium complex **10b** shows two waves between −0.2 and −1.4 V with $E_{1/2}$'s of −1.036 and −1.137 V, respectively. The ratio of the limiting currents is unequal to 1 (0.60 and 0.78 μA, respectively).[25] The cyclic voltammograms at scan rates of 0.5–6 V/s are shown in Figure 2.

This reduction/oxidation process is *chemically reversible*, because when five scans at scan rates of 0.5 and 6 V/s were applied, five identical cyclic voltammograms were recorded. It will be obvious that other phenomena than simple reduction and oxidation must be involved. Based on these experiments both adsorption of the oxidized and reduced forms is assumed.[27]

(23) Hughes, D. L.; Mortimer, C. L.; Truter, M. R. *Acta Crystallogr., Sect. B* **1978**, *34*, 800.

(24) Zollinger, D. P.; Bos, M.; van Veen-Blaauw, A. M. W.; van der Linden, W. E. *Anal. Chim. Acta* **1985**, *167*, 89.

(25) Determination of the half-wave potentials ($E_{1/2}$) was done manually. The slopes were estimated with $E_{1/4} - E_{3/4}$. The peak at about −0.3 V, which occurs at higher scan rates, is probably due to capacitance effects. This peak is also found in the blank.

(26) (a) *Handbook of Chemistry and Physics*, 64th ed.; CRC Press, Inc.: Boca Raton, FL, 1983. (b) March, J. *Advanced Organic Chemistry*, 3rd ed.; John Wiley and Sons: New York, 1985. (c) Bovill, M. J.; Chadwick, D. J.; Sutherland, I. O.; Watkin, D. *J. Chem. Soc., Perkin Trans. 1* **1980**, 1529. (d) Bernardi, F.; Csizmadia, I. G.; Mangini, A., Eds. *Studies in Organic Chemistry, Vol 19; Organic Sulfur Chemistry: Theoretical and Experimental Advances*; Elsevier: Amsterdam, 1985; pp 68–132.

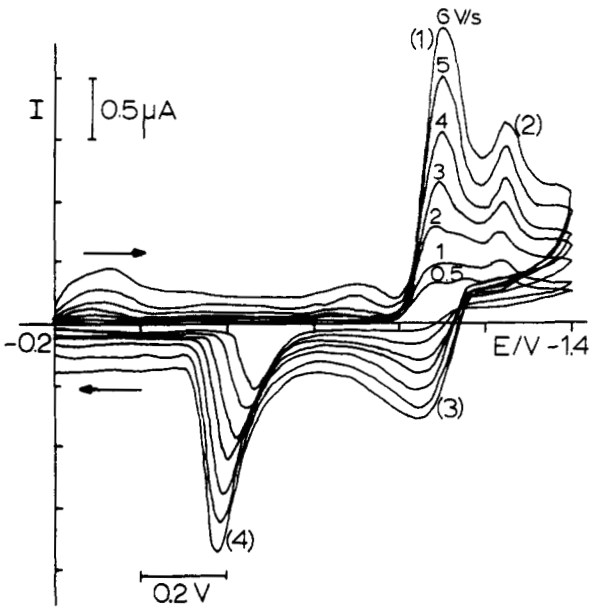

Figure 2. Cyclic voltammograms of **10b** in DMSO at scan rates of 0.5–6 V/s. Peak 1: Ox + 2e → Red^{2-}. Peak 2: Ox_{ads} + 2e → Red^{2-}_{ads}. Peak 3: Red^{2-} → Ox_{ads} + 2e. Peak 4: Red^{2-}_{ads} → Ox + 2e.

These assumptions are supported further by both cyclic voltammetry and Kalousek polarography. When cyclic voltammograms between −0.2 and −1.2 V were recorded with a scan rate of 2 V/s peak 3 and 4 have almost equal heights. At a scan rate of 6 V/s peak 3 is even higher than peak 4. This is consistent with the proposed adsorption effects, because the adsorbed oxidized form is still present and there is less time for adsorption of the reduced form, that is produced in a smaller amount. When in a scan (2 V/s) from −0.2 to −1.4 the potential was kept at −1.4 V for about 3 s, peak 3 was absent and peak 4 was largely increased. When in a scan (2 V/s) from −0.2 to −1.4 V the potential was kept at −1.2 for about 3 s, peak 2 was a little smaller, peak 3 decreased, and peak 4 largely increased. Because of the hold at a potential at which reduction takes place the oxidized form near the electrode surface will be exhausted and only the reduced form will be present, which is adsorbed in larger amounts at the mercury drop.

From Kalousek polarography further evidence was obtained for the proposed mechanism. Both K_1 (measurement of the current at the pulse top) and K_2 (measurement of the current at the pulse base) type experiments were performed. The applied pulse frequencies were 5, 25, 50, 150, and 300 Hz. When K_1 type polarograms were recorded between −0.8 and −1.4 V with the pulse base at −0.8 V, two waves were observed. The second wave became relatively larger and shows a maximum more cathodic than −1.2 V upon increasing the pulse frequency. The K_2 type measurements showed the same behavior. This is in agreement with the assumption that the second reduction is the reduction of the adsorbed oxidized form. These results clearly show that adsorption phenomena play a role. When K_2 type measurements between −0.8 and −1.4 V were performed with the pulse base at −1.4 V, virtually no wave was observed. During the pulse base the adsorbed reduced form is produced at the electrode surface which cannot be reoxidized in the potential region of −0.8 to −1.4 V. When K_2 type experiments were performed with the pulse base at −1.2 V the polarograms show a wave, anodic of −1.2 V.

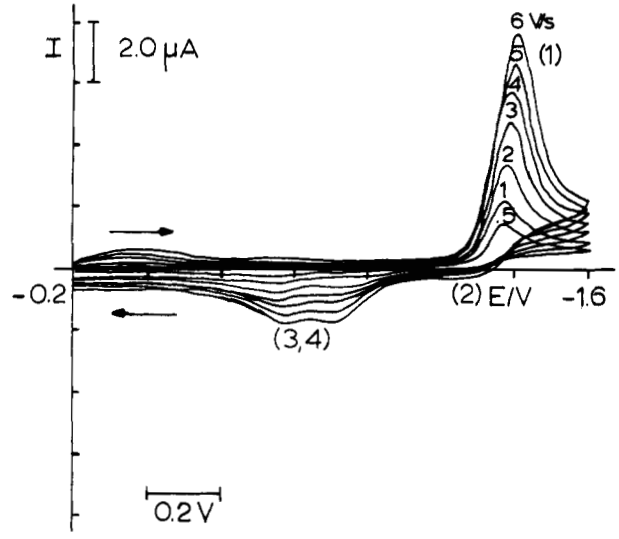

Figure 3. Cyclic voltammograms of **10e** in DMSO at scan rates of 0.5–6 V/s. Peak 1: Ox + 2e → Red^{2-}_{ads}. Peak 2: Red^{2-} → Ox + 2e. Peak 3, 4: Red^{2-}_{ads} → Ox + 2e.

This is consistent with the production of the reduced form in solution which is reoxidized via peak 3. These results are comparable with the cyclic voltammetry in which holds at −1.2 and −1.4 V were applied and the oxidation peak 3 was no longer observed. When K_1 type polarograms were recorded between −0.4 and −1.4 V with pulse bases at −1.2 and −1.4 V a maximum at a more anodic potential than −0.8 V was observed that shifted to a more anodic value upon increasing the pulse frequency. This demonstrates that for peak 4 in the cyclic voltammograms adsorption phenomena play a role and that it can be assigned to the reoxidation of the adsorbed reduced form. Another indication for this is that the peak potential of peak 4 is scan rate dependent.[28]

The dinickel/cesium complex **10e** shows one wave in the DC_T polarogram between −0.2 and −1.6 V, with an $E_{1/2}$ of −1.300 V and a slope of 61 mV. Potentiostatic electrolysis at −1.6 V resulted in a current-time curve with exponential shape and when the current was at the background level, two electrons per complex were transferred. The cyclic voltammograms at scan rates of 0.5–6 V/s are shown in Figure 3.

Repeated scans at 6 V/s resulted in identical cyclic voltammograms, which leads to the conclusion that this reduction/oxidation is *chemically reversible*. Peak 2 disappears when in scans at 2 and 6 V/s a hold for several seconds was applied at −1.6 V, the peaks 3 and 4 are enhanced. These results may be explained by assuming that the reduced form (Red^{2-}) is adsorbed at the mercury surface. Oxidation of the reduced form, near the electrode surface, occurs at peak 2 and oxidation of the adsorbed reduced form occurs at the peaks 3 and 4. No explanation is found for the occurrence of two oxidation peaks of the adsorbed form.

The DC_T polarogram of the dinickel/barium complex **10h** (0.51 mM) shows three waves between −0.2 and −1.6 V with $E_{1/2}$'s of −0.995, −1.162, and −1.329 V, respectively. The ratio of the limiting currents is about 1:1.2:1.1. The same measurement at a concentration of 0.44 mM also gave a DC_T polarogram with three waves at virtually the same $E_{1/2}$'s, but the ratio of the limiting currents is 1:1.1:2.1. We assigned the first wave to the reduction of the oxidized form to the adsorbed reduced form, the second wave to

(27) Heyrovski, J.; Kuta, J. *Grundlagen der Polarographie*; Akademie-Verlag: Berlin, 1965.

(28) Bond, A. M. *Modern Polarographic Methods in Analytical Chemistry*; Marcel Dekker, Inc.: New York, 1980.

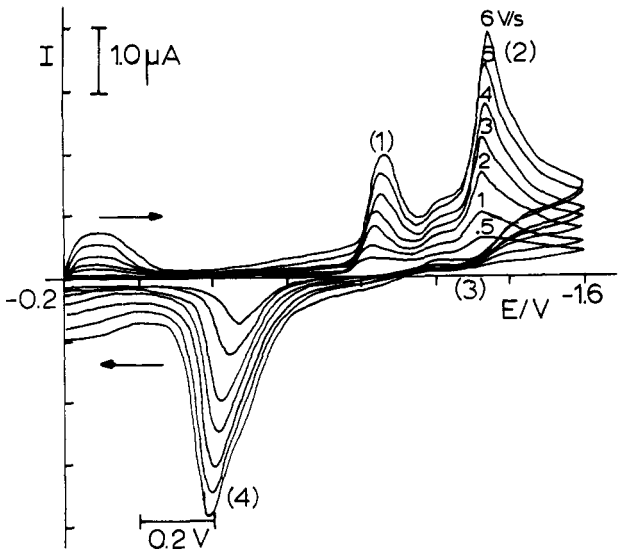

Figure 4. Cyclic voltammograms of **10h** in DMSO at scan rates of 0.5–6 V/s. Peak 1: Ox + 2e → Red^{2-}_{ads}. Peak 2: Ox_{ads} + 2e → Red^{2-}. Peak 3: Red^{2-} → Ox_{ads} + 2e. Peak 4: Red^{2-}_{ads} → Ox + 2e.

the reduction of the oxidized form to the reduced form, and the third wave to the reduction of the adsorbed oxidized form to the reduced form. These assignments are supported by cyclic voltammetry. The cyclic voltammograms at scan rates of 0.5–6 V/s are shown in Figure 4.

This reduction/oxidation process is *chemically reversible* as was concluded from repeated scans at a scan rate of 6 V/s, which show identical cyclic voltammograms. Peak 3 is absent and peak 4 is enhanced when in a scan at 6 V/s between −0.2 and −1.6 V a hold was applied at −1.6 V for several seconds. In a scan at 6 V/s between −0.2 and −1.2 V peak 1 and a decreased peak 4 were observed. When in a scan at 6 V/s between −0.2 and −1.2 V a hold was applied at −1.2 V for several seconds, peak 4 was increased. When repeated scans were applied at a scan rate of 6 V/s between −0.9 and −1.6 V the peaks 1 and 2 are decreased, and in between these peaks a new peak appeared. This observation supports the conclusions about the three waves in the DC_T polarogram. From the above mentioned observations it can be concluded that, similar to the reduction/oxidation behavior of compound **10a**, here adsorption phenomena of both the oxidized and reduced form also take place.

EPR Spectroscopy. Given the unique trinuclear structure with two salophen units in the solid state and the electrochemical evidence that the two transition-metal cations M_1 are communicating and the fact that they most likely cannot be reduced independently, it was decided to study the frozen-solution EPR spectra of the dicopper containing complexes **10a**, **10d**, and **10g**. Analysis of EPR spectra of dinuclear copper(II) systems is well documented[29] for both antiferromagnetic and ferromagnetic dinuclear compounds with each of the metal cations having $S = {}^1/_2$.

The spectra in solution of the compounds **10a** and **10g**, containing the $BaCu_2$ unit show resonances typical for $S = 1$, and a typical spectrum (compound **10a**) is shown in Figure 5.

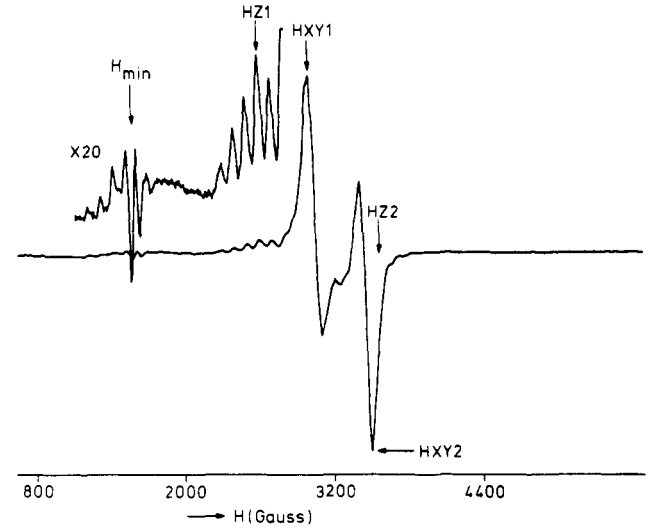

Figure 5. Frozen EPR spectrum of **10a** in MeOH; assignment of some of the peaks is indicated in the drawing.

Bands at $\Delta m = 2$ (so-called half-field line) with a Cu hyperfine splitting of 95 (2) G and some bands in the $\Delta m = 1$ region with the same value for this hyperfine splitting are indicative for Cu(II) dimers with a small zero-field splitting. Due to the fact that the electron spin is coupled with 2 Cu nuclei, each having m_I of ${}^3/_2$, seven lines are observed ($2 \times 3 + 1$) and the A value is half the value reported for Cu(II) in a square-planar CuN_2O_2 chromophore. This observation confirms that both Cu(II) cations are communicating with each other, in agreement with the electrochemical results.

The spectrum of the cesium/dicopper complex **10d**, on the other hand, shows a broad band near $g = 2$, with only some weak features for $S = 1$ at 3400 G and at half field. This suggests that the structure of the molecule in MeOH solution is less stable than that of the barium analogue and that only a small fraction is present in the folded conformation with close Cu–Cu contact. Also the electrochemical measurements already indicated that the communication between the Cu cations in the dicopper/cesium complex **10d** is less straightforward than for the dicopper/barium complex **10a**.

The spectra of both dicopper/barium complexes **10a** and **10g** are almost the same although the bands are better resolved for compound **10a**; therefore, compound **10a** has been used for a detailed analysis of the EPR spectrum in glassy state (frozen MeOH).

The intensity of X-band frequencies of the $\Delta m = 1$ signal compared to the half-field line signal (called I_r), which is about 100 (20), can be used to determine the spin-spin distance, using the empirical formula of Eaton:[29c,d] r^6 (in Å) = $20I_r$. This results in a distance of 3.6 (2) Å for the Cu–Cu distance, in nice–though not very accurate–agreement with the solid-state distance of 3.50 Å.

The high spectral resolution of the lines near $g = 2$ allows the calculation of the g values and the zero-field splitting of the triplet state. Using the known formula[29a,b] we arrive at $g_\parallel = 2.16$ (1), $A_\parallel = 95$ (2) G, $g_\perp = 2.04$ (1), and $D = 410$ (10) G (this corresponds to 0.039 cm^{-1}). The value of $A_\parallel$ is just about 50% of the value observed for the corresponding copper/barium complex,[15a] as one would expect for coupled dinuclear systems. The lower value of $g_\parallel$ compared to the corresponding copper/barium species[15a] ($g_\parallel = 2.21$) probably indicates a higher degree of covalency (electron delocalization of the unpaired electron into the salophen unit). As a matter of fact, the observed spectrum

(29) (a) Reedijk, J.; Knetsch, D.; Nieuwenhuyse, B. *Inorg. Chim. Acta* **1971**, *5*, 568 and references cited in there. (b) Mesa J. L.; Rojo, T.; Arriortua, M.; Villeneuve, G.; Folgado, J. V.; Beltrán-Porter, A.; Beltrán-Porter, D. *J. Chem. Soc., Dalton Trans.* **1989**, 53. (c) Eaton, S. S.; More, K. M.; Sawant, B. H.; Eaton, G. R. *J. Am. Chem. Soc.* **1983**, *105*, 6560. (d) Eaton, S. S., Eaton, G. R. *J. Am. Chem. Soc.* **1982**, *104*, 5002.

and the derived parameters correspond very well with those of the frozen-solution dinuclear structure of $[Cu(dmgH)_2]_2$.[30]

The EPR spectra give no information about the value of magnetic exchange coupling parameter for the two unpaired electrons; such coupling (called J) is usually very small, and the determination would require measurements of the magnetic susceptibility down to very low temperatures (<4 K), which is left for future investigations on the present and other compounds.

Assuming only dipolar contributions to the observed EPR zero-field splitting, the empirical formula: $D_{dd} = 0.65g_z^2/r^3$ (D in cm^{-1} and r in Å), would yield a separation of 4.3 (1) Å for the two spins of $S = {}^1/_2$, which is significantly larger than the solid-state Cu–Cu distance of 3.5 Å. The small dipolar contribution to the zero-field splitting might be due to electron delocalization (covalency) of the unpaired electron into the salophen unit.[31] This delocalization would easily account for the somewhat larger dipole-dipole separation; a covalency delocalization correction on the distance (of about 0.5 Å) has been reported for related dinuclear Cu species, like the above mentioned $[Cu(dmgH)_2]_2$ and $Cu_2(tartrate)_4$.[31] Moreover, such a delocalization is known to be present in similar mononuclear Cu salophen compounds.[30]

To find out whether or not the "stacking" of the two halves of the molecule can be broken up in solution by addition of bridge-forming ligands, the MeOH solution of the dicopper/barium complex **10a** was treated with varying amounts of F^- and Im^- (imidazolate) and possible product formation was followed with EPR. Up to 30-fold excesses of both ligands, no changes in the dinuclear $S = 1$ signals were found.

These results clearly indicate that the structures in solution of this type of Cu_2Ba trinuclear species are stable and most likely are the same as found for the solid-state X-ray crystal structure.

Conclusions

The metal cation templated (2 + 2) macrocyclization of the dialdehydes **3a** and **3b** with the diamine **8** offers a convenient route to heterotrinuclear metal complexes. For the cyclization of the dialdehyde **3a** both Ba^{2+} and Cs^+ proved suitable template ions, but the dialdehyde **3b** could only be cyclized with Ba^{2+} as template ion. The three crystal structures clearly show that by cocomplexation of a hard cation (Ba^{2+}) the two salophen units are brought into close proximity. Short distances between the two transition-metal cations were observed (3.42 and 3.50 Å). The electrochemistry of the copper-containing heterotrinuclear complexes **10a**, **10d**, and **10g** shows that there is an interaction between the two copper cations, which is the strongest and most stable for the dicopper/barium complex **10a**. It is therefore likely that also in solution the conformation is folded, similar to the structure in the solid state. The electrochemical behavior of the nickel-containing heterotrinuclear complexes **10b**, **10e**, and **10h** is complicated by adsorption phenomena at the mercury electrode. Significant differences due to variation in the hard cation and structural variation in the ligand have been observed for both the copper- and nickel-containing heterotrinuclear complexes.

The EPR spectra of the copper-containing trinuclear complex **10a**, **10d**, and **10g** in MeOH solution are in agreement with the electrochemical results and confirm that the conformation of the molecules remains intact. Event the addition of exogenous ligands, which might bridge the two Cu(II) cations, does not change the EPR spectra, proving that the structures do not change under these circumstances. Only in the case of the dicopper/cesium complex **10d** partial decomposition of the dimer has been found in MeOH.

The value of the zero-field splitting parameter D leads to a dipolar distance of 4.3 (2) Å for the two $S = {}^1/_2$ systems, whereas the relative intensities of $\Delta m = 2$ and $\Delta m = 1$ signals yield a distance of 3.6 (2) Å. These larger distances suggest that the unpaired electrons are not completely located on Cu(II), but as a result of covalency are delocalized over the salophen units.

In conclusion we can state that we have demonstrated that in the macrocycles **10a–h** two soft metal cations can be brought into *close proximity in a unique way* as proven by X-ray crystallography, electrochemistry, and EPR spectroscopy.

Structural variation in both the crown ether cavity for hard cations as well as in the chelate moieties for the soft cations are in progress. Future work will also be dealing with detailed studies of the EPR intensities and magnetic susceptibility as a function of the temperature.

Experimental Section

FAB mass spectra were recorded using *m*-nitrobenzyl alcohol as matrix. Elemental analyses and Karl-Fischer titrations were carried out by the Department of Chemical Analysis of our institute.

All chemicals were reagent grade and used without further purification. DIP refers to diisopropyl ether, DMSO to dimethyl sulfoxide, and THF to tetrahydrofuran. Dropwise addition over a period of several hours was always carried out with a perfusor.

Ar refers to the aromatic ring with a "precursor" aldehyde moiety; Ar′ refers to the aromatic ring with the two imine bonds.

3,3′-[Oxybis(2,1-ethanediyloxy)]bis(2-hydroxybenzaldehyde) (3a). To a suspension of NaH (2.64 g, 0.088 mol) under nitrogen in 20 mL of DMSO was added dropwise a solution of 2,3-dihydroxybenzaldehyde (**1**, 5.56 g, 0.040 mol) in 20 mL of DMSO. The temperature was kept under 25 °C. After the addition was completed the resulting brown solution was stirred for 1 h. Subsequently a solution of the ditosylate **2** (3.84 g, 0.020 mol) in 20 mL of DMSO was added in one portion. After stirring for 20 h 500 mL of water was added, and the aqueous layer was acidified with 6 M HCl to pH 2. This layer was extracted with $CHCl_3$ (5 × 100 mL) and the combined organic layers were well washed with 1 M HCl. After drying with $MgSO_4$ the solvent was removed and the residue was purified by column chromatography (silica gel, $CHCl_3$) to give **3a** as a pale yellow solid: yield 49%; mp 75 °C (MeOH); ^1H NMR ($CDCl_3$) δ 10.89 (s, 2 H, OH), 9.94 (s, 2 H, CHO), 7.3–6.8 (m, 6 H, Ar H), 4.3–4.2 (m, 4 H, Ar OCH_2), 4.0–3.9 (m, 4 H, OCH_2); ^{13}C NMR ($CDCl_3$) δ 196.0 (d, CHO), 152.1, 147.3 (s, Ar C-2,3), 125.0, 120.7, 119.5 (d, Ar C-4–6), 121.3 (s, Ar C-1), 69.9, 69.2 (t, OCH_2); IR (KBr) 1654 (C=O) cm^{-1}; mass spectrum, m/e 346.106 (M^+, calcd 346.105). Anal. Calcd for $C_{18}H_{18}O_7 \cdot CH_3OH$: C, 60.31; H, 5.86. Found: C, 60.45; H, 5.56.

3-(2-Bromoethoxy)-2-(2-propenyloxy)benzaldehyde (5). A mixture of compound **4** (17.02 g, 0.096 mol), 1,2-dibromoethane (200 g, 1 mol), and K_2CO_3 (20.00 g, 0.14 mol) in 250 mL of CH_3CN was refluxed for 20 h. The mixture was cooled to room temperature, and the salts were filtered off. The filtrate was evaporated to dryness, and the residue was purified by column chromatography (silica gel, $CHCl_3$). Compound **5** was obtained as an oil which slowly solidified upon standing: yield 98%; mp 35–36 °C; ^1H NMR ($CDCl_3$) δ 10.26 (s, 1 H, CHO), 7.5–7.0 (m, 3 H, Ar H), 6.3–5.8 (m, 1 H, =CH), 5.6–5.2 (m, 2 H, $=CH_2$), 4.73 (dd, 2 H, J = 4.4 and 1.1 Hz, $OCH_2CH=$), 4.37 (t, 2 H, J = 6.0 Hz, OCH_2), 3.69 (t, 2 H, J = 6.0 Hz, CH_2Br); ^{13}C NMR ($CDCl_3$) δ 190.2 (d, CHO), 151.5 (s, Ar C-2,3), 133.0 (d, =CH), 130.4 (s, Ar C-1), 124.1, 120.1, 119.6 (d, Ar C-4–6), 119.1 (t, $=CH_2$), 75.5 (t, $OCH_2CH=$), 68.9 (t, OCH_2), 29.1 (t, CH_2Br); IR (KBr) 1686

(30) (a) O'Brien, P. *Coord. Chem. Rev.* **1984**, *55*, 169. (b) Wiersma, A. K.; Windle, J. J. *J. Phys. Chem.* **1964**, *68*, 2316.

(31) (a) Chasteen, N. D.; Belford, R. L. *Inorg. Chem.* **1970**, *9*, 169. (b) Villa, J. F.; Hatfield, W. E. *Inorg. Nucl. Chem. Lett.* **1970**, *6*, 511.

(C=O) cm^{-1}; mass spectrum, m/e 284.003 (M^+, calcd 284.005). Anal. Calcd for $C_{12}H_{13}BrO_3$: C, 50.55; H, 4.60. Found: C, 50.80; H, 4.86.

2-[3-(2-Bromoethoxy)-2-(2-propenyloxy)phenyl]-1,3-dioxolane (6). A solution of **5** (26.69 g, 0.081 mol), ethylene glycol (5.81 g, 0.126 mol), and a catalytic amount of *p*-TsOH in 500 mL of toluene was refluxed for 20 h. Water was removed with a Dean–Stark trap. The solution was cooled to room temperature and was washed with a saturated solution of $NaHCO_3$ and brine. After drying with $MgSO_4$ the toluene was evaporated, and the residue was purified by column chromatography (silica gel, $CHCl_3$) to give **6** as pale yellow oil: yield 96%; ^1H NMR ($CDCl_3$) δ 7.3–6.9 (m, 3 H, Ar H), 6.4–5.9 (m, 1 H, =CH), 6.13 (s, 1 H, Ar CH), 5.6–5.1 (m, 2 H, $=CH_2$), 4.73 (dd, 2 H, J = 4.4 and 1.1 Hz, $OCH_2CH=$), 4.37 (t, 2 H, J = 6.0 Hz, OCH_2), 4.1–4.0 (m, 4 H, OCH_2CH_2O), 3.69 (t, 2 H, J = 6.0 Hz, CH_2Br); ^{13}C NMR ($CDCl_3$) δ 150.7, 146.8 (s, Ar C-2,3), 145.1 (s, Ar C-1), 134.0 (d, =CH), 123.7, 119.3, 114.9 (d, Ar C-4–6), 117.3 (t, $=CH_2$), 99.1 (d, Ar *C*H), 74.5 (t, $OCH_2CH=$), 68.6 (t, OCH_2), 65.0 (t, OCH_2CH_2O), 29.4 (t, CH_2Br); mass spectrum, m/e 328.0 (M^+, calcd for $C_{14}H_{17}{}^{79}BrO_4$ 328.0).

2,2′-[Thiobis[2,1-(ethanediyloxy)-3,1-[2-(2-propenyloxy)]phenylene]]bis(1,3-dioxolane) (7). A solution of **6** (28.92 g, 0.088 mol) and 0.5 equiv of Na_2S in 300 mL of MeOH was refluxed for 20 h, after which it was cooled to room temperature and the solvent was evaporated. To the residue was added 100 mL of $CHCl_3$. Subsequently the organic layer was washed with a $NaHCO_3$ solution and brine, after which it was dried with $MgSO_4$. The solvent was removed, and the residue was purified by column chromatography (Al_2O_3, ethyl acetate–hexane = 35:65), which afforded **7** as a slightly yellow oil: yield 84%; ^1H NMR ($CDCl_3$) δ 7.3–6.9 (m, 6 H, Ar H), 6.4–5.9 (m, 2 H, =CH), 6.13 (s, 2 H, Ar CH), 5.6–5.1 (m, 4 H, $=CH_2$), 4.73 (dd, 4 H, J = 4.4 and 1.1 Hz, $OCH_2CH=$), 4.37 (t, 4 H, J = 6.0 Hz, OCH_2), 4.1–4.0 (m, 8 H, OCH_2CH_2O), 3.02 (t, 4 H, J = 6.0 Hz, SCH_2); ^{13}C NMR ($CDCl_3$) δ 151.6, 151.4 (s, Ar C-2,3), 134.3 (d, =CH), 132.1 (s, Ar C-1), 123.9, 119.2, 115.0 (d, Ar C-4–6), 117.2 (t, $=CH_2$), 99.5 (d, Ar *C*H), 74.5 (t, $OCH_2CH=$), 68.8 (t, OCH_2), 65.2 (t, OCH_2CH_2O), 31.9 (t, SCH_2); mass spectrum, m/e 530.1 (M^+, calcd for $C_{28}H_{34}O_8S$ 530.0).

3,3′-[Thiobis(2,1-ethanediyloxy)]bis(2-hydroxybenzaldehyde) (3b). A mixture of **7** (2.00 g, 4.26 mmol), CH_3COOH (6.60 g, 0.11 mol), and SeO_2 (7.71 g, 0.70 mol) in 50 mL of dioxane was refluxed for 1 h. The mixture was cooled to room temperature and filtered. The filtrate was diluted with 400 mL of water and extracted with $CHCl_3$ (4 × 50 mL). The combined organic layers were washed once with brine (100 mL) and dried with $MgSO_4$. The solvent was removed, and the residue was purified by column chromatography (silica gel, hexane–ethyl acetate = 65:35) to give **3b** as a yellow solid: yield 16%; mp 96–98 °C; ^1H NMR ($CDCl_3$) δ 10.97 (s, 2 H, OH), 9.91 (s, 2 H, CHO), 7.3–7.0 (m, 6 H, Ar H), 4.37 (t, 4 H, J = 6.0 Hz, OCH_2), 3.17 (t, 4 H, J = 6.0 Hz, SCH_2); ^{13}C NMR ($CDCl_3$) δ 196.4 (d, CHO), 152.2, 147.0 (s, Ar C-2,3), 125.4, 120.6, 119.5 (d, Ar C-4–6), 121.0 (s, Ar C-1), 69.6 (t, OCH_2), 31.6 (t, SCH_2); IR (KBr) 1648 (C=O) cm^{-1}. Anal. Calcd for $C_{18}H_{18}O_6S$: C, 59.66; H, 5.01. Found: C, 59.53; H, 4.96.

General Procedure for the Synthesis of the Complexes 9b, 9c, and 9e. To a refluxing solution of $Ba(CF_3SO_3)_2$ (0.23 g, 0.52 mmol) or $Cs(CF_3SO_3)$ (0.15 g, 0.52 mmol) in 100 mL of MeOH were added simultaneously a solution of 2 equiv of the dialdehyde **3** (1.04 mmol) in 25 mL of THF and a solution of *o*-phenylenediamine (**8**, 0.56 g, 1.04 mmol) in 25 mL of MeOH over a period of 2 h. The resulting colored solution was cooled to room temperature and concentrated to 20 mL, and after the addition of some DIP the product crystallized. It was filtered off and dissolved in 50 mL of MeOH. The MeOH layer was filtered in order to remove some of the remaining noncyclic reaction products. The filtrate was concentrated to dryness. In the case of **9b** the residue was dissolved in MeOH and carefully precipitated with petroleum ether (bp 40–60 °C). In the other cases the residue was washed with DIP.

[13,14,16,17,38,39,41,42-Octahydro-7,11:19,23:32,36:44,48-tetramethenodibenzo[*o*,*l*$_1$][1,4,7,24,27,30,14,17,37,40]-hexaoxatetraazacyclohexatetracontin-51,52,53,54-tetrol-*O*^{12},*O*^{15},*O*^{18},*O*^{37},*O*^{40},*O*^{43},*O*^{51},*O*^{52},*O*^{53},*O*^{54}]barium(2+) bis(trifluoromethanesulfonate) (9b): red solid; yield 63%; mp 270–280 °C dec; ^1H NMR (DMSO-d_6) δ 13.37 (s, 4 H, OH), 8.92 (s, 4 H, N=CH), 7.45 (s, 8 H, Ar′ H), 7.3–7.1 (m, 8 H, Ar H), 6.9–6.7 (m, 4 H, Ar H), 4.1–4.0 (m, 8 H, Ar OCH_2), 4.0–3.9 (m, 8 H, OCH_2); ^{13}C NMR (DMSO-d_6) δ 163.5 (d, N=C), 151.4 (s, Ar C-3), 146.4 (s, Ar C-2), 140.7 (s, Ar′ C-1), 127.3, 124.2, 118.7, 117.6, 117.3 (d, Ar C-4–6, Ar′ C-2,3), 118.6 (s, Ar C-1), 68.5, 67.8 (t, OCH_2); IR (KBr) 1620 (N=C) cm^{-1}; FAB mass spectrum, m/e 1123 [(M − CF_3SO_3)$^+$, calcd 1123]. Anal. Calcd for $C_{50}H_{44}BaF_6N_4O_{16}S_2$: C, 47.20; H, 3.49; N, 4.40. Found: C, 46.96; H, 3.49; N, 4.20.

[13,14,16,17,38,39,41,42-Octahydro-7,11:19,23:32,36:44,48-tetramethenodibenzo[*o*,*l*$_1$][1,4,7,24,27,30,14,17,37,40]-hexaoxatetraazacyclohexatetracontin-51,52,53,54-tetrol-*O*^{12},*O*^{15},*O*^{18},*O*^{37},*O*^{40},*O*^{43},*O*^{51},*O*^{52},*O*^{53},*O*^{54}]cesium(1+) trifluoromethanesulfonate (9c): orange solid; yield 69%; mp 140–142 °C; ^1H NMR (DMSO-d_6) δ 13.50 (br s, 4 H, OH), 8.80 (s, 4 H, N=CH), 7.43 (s, 8 H, Ar′ H), 7.3–7.0 (m, 8 H, Ar H), 6.9–6.6 (m, 4 H, Ar H), 4.3–4.1 (m, 8 H, Ar OCH_2), 4.0–3.8 (m, 8 H, OCH_2); IR (KBr) 1613 (N=C) cm^{-1}; FAB mass spectrum, m/e 970 [(M − CF_3SO_3 + H)$^+$, calcd 970]. Anal. Calcd for $C_{49}H_{44}CsF_3N_4O_{13}S\cdot 1.3H_2O$: C, 51.52; H, 4.11; Cs, 11.6; N, 4.90. Found: C, 51.63; H, 4.10; Cs, 11.2; N, 5.13. Karl–Fisher titration calcd for $1.3H_2O$: H_2O, 2.02. Found: H_2O, 2.05.

[13,14,16,17,38,39,41,42-Octahydro-7,11:19,23:32,36:44,48-tetramethenodibenzo[*o*,*l*$_1$][1,7,24,30,4,27,14,17,37,40]-tetraoxadithiatetraazacyclohexatetracontin-51,52,53,54-tetrol-*O*^{12},*O*^{18},*O*^{37},*O*^{43},*O*^{51},*O*^{52},*O*^{53},*O*^{54},*S*^{15},*S*^{40}]barium(2+) bis(trifluoromethanesulfonate) (9e): orange solid; yield 45%; mp 291 °C dec; ^1H NMR (Nicolet NT-200 WB spectrometer) (DMSO-d_6) δ 13.29 (s, 4 H, OH), 8.94 (s, 4 H, N=CH), 7.5–7.4 (m, 8 H, Ar′ H), 7.3–7.2 (m, 4 H, Ar H), 7.1–7.0 (m, 4 H, Ar H), 6.9–6.8 (m, 4 H, Ar H), 4.19 (t, 8 H, J = 5.8 Hz, OCH_2), 3.08 (t, 8 H, J = 5.8 Hz, SCH_2); IR (KBr) 1621 (C=N) cm^{-1}; FAB mass spectrum, m/e 1155 [(M − CF_3SO_3)$^+$, calcd 1155]. Anal. Calcd for $C_{50}H_{44}BaF_6N_4O_{14}S_4\cdot H_2O$: C, 45.41; H, 3.51; N, 4.24. Found: C, 45.30; H, 3.43; N, 4.01.

General Procedure for the Synthesis of the Trinuclear Complexes 10a–h. To a solution of the complexes **9** (6.00 mmol) in 30 mL of MeOH a solution of 2 equiv of copper, nickel, or zinc acetate in MeOH was added in one portion. The solution was warmed at 50 °C for 0.5 h. After cooling to room temperature the solution was concentrated to 5 mL and subsequently 25 mL of DIP was added. The trinuclear complex crystallized and was filtered off and was washed once with DIP. The solid residue was dissolved in a mixture of MeOH and CH_3CN (1:1), and some Et_2O was added carefully after which the trinuclear complex crystallized. It was filtered off and dried.

[μ_3-[13,14,16,17,38,39,41,42-Octahydro-7,11:19,23:32,36:44,48-tetramethenodibenzo[*o*,*l*$_1$][1,4,7,24,27,30,14,17,37,40]-hexaoxatetraazacyclohexatetracontin-51,52,53,54-tetrolato(4−)-*N*^{5},*N*^{50},*O*^{51},*O*^{54}:*N*^{25},*N*^{30},*O*^{52},*O*^{53}:*O*^{12},*O*^{15},*O*^{18},*O*^{37},*O*^{40},*O*^{43},*O*^{51},*O*^{52},*O*^{53},*O*^{54}]bis(copper)]barium(2+) bis(trifluoromethanesulfonate) (10a): green solid; yield 74%; mp >300 °C; IR (KBr) 1608 (N=C) cm^{-1}; FAB mass spectrum, m/e 1245 [(M − CF_3SO_3)$^+$, calcd 1245]. Anal. Calcd for $C_{50}H_{40}BaCu_2F_6N_4O_{16}S_2\cdot 2H_2O$: C, 41.95; H, 3.10; N, 3.91. Found: C, 42.05; H, 3.02; N, 4.13.

[μ_3-[13,14,16,17,38,39,41,42-Octahydro-7,11:19,23:32,36:44,48-tetramethenodibenzo[*o*,*l*$_1$][1,4,7,24,27,30,14,17,37,40]-hexaoxatetraazacyclohexatetracontin-51,52,53,54-tetrolato(4−)-*N*^{5},*N*^{50},*O*^{51},*O*^{54}:*N*^{25},*N*^{30},*O*^{52},*O*^{53}:*O*^{12},*O*^{15},*O*^{18},*O*^{37},*O*^{40},*O*^{43},*O*^{51},*O*^{52},*O*^{53},*O*^{54}+]bis(nickel)]barium(2+) bis(trifluoromethanesulfonate) (10b): dark red solid; yield 64%; mp >300 °C; ^1H NMR (DMSO-d_6) δ 8.39 (s, 4 H, N=CH), 7.7–7.5 (m, 4 H, Ar′ H), 7.2–7.0 (m, 4 H, Ar′ H), 7.0–6.6 (m, 4 H, Ar H), 6.5–6.3 (m, 8 H, Ar H), 4.9–3.6 (m, 16 H, OCH_2); ^{13}C NMR (DMSO-d_6) δ 156.9 (d, N=C), 151.6 (s, Ar C-3), 147.3 (s, Ar C-2), 140.7 (s, Ar′ C-1), 127.7, 125.1, 115.6, 115.3, 113.7 (d, Ar C-4–6, Ar′ C-2,3), 119.4 (s, Ar C-1), 67.3, 66.2 (t, OCH_2); IR (KBr) 1610 (N=C) cm^{-1}; FAB mass spectrum, m/e 1234 [(M − CF_3SO_3)$^+$, calcd 1234]. Anal. Calcd for $C_{50}H_{40}BaF_6N_4Ni_2O_{16}S_2\cdot 2H_2O$: C, 42.24; H, 3.12; N, 3.94. Found: C, 41.91; H, 3.16; N, 3.85.

[μ_3-[13,14,16,17,38,39,41,42-Octahydro-7,11:19,23:32,36:44,48-tetramethenodibenzo[*o*,*l*$_1$][1,4,7,24,27,30,14,17,37,40]-hexaoxatetraazacyclohexatetracontin-51,52,53,54-tetrolato(4−)-*N*^{5},*N*^{50},*O*^{51},*O*^{54}:*N*^{25},*N*^{30},*O*^{52},*O*^{53}:*O*^{12},*O*^{15},*O*^{18},*O*^{37},

$O^{40},O^{43},O^{51},O^{52},O^{53},O^{54}$]bis(zinc)]barium(2+) bis(trifluoromethanesulfonate) (10c): yellow solid; yield 55%; mp >300 °C; ^{1}H NMR (DMSO-d_6) δ 8.48 (s, 4 H, N=CH), 7.6–7.3 (m, 8 H, Ar' H), 6.9–6.7 (m, 4 H, Ar H), 6.5–6.2 (m, 8 H, Ar H), 4.4–3.9 (m, 16 H, OCH_2); ^{13}C NMR (DMSO-d_6) δ 161.5 (d, N=C), 160.8 (s, Ar C-3), 150.5 (s, Ar C-2), 137.5 (s, Ar' C-1), 127.7, 126.9, 115.9, 113.5, 113.3 (d, Ar C-4–6, Ar' C-2,3), 118.9 (s, Ar C-1), 68.7, 66.5 (t, OCH_2); IR (KBr) 1609 (N=C) cm^{-1}; FAB mass spectrum, m/e 1249 [(M - CF_3SO_3)$^+$, calcd 1249]. Anal. Calcd for $C_{50}H_{40}F_6N_4O_{16}S_2Zn_2\cdot 3.3H_2O$: C, 41.33; H, 3.19; N, 3.86. Found: C, 41.38; H, 3.01; N, 3.77. Karl–Fisher titration calcd for $3.3H_2O$: H_2O, 4.08. Found: H_2O, 4.06.

[μ_3-[13,14,16,17,38,39,41,42-Octahydro-7,11:19,23:32,36:44,48-tetramethenodibenzo[o,l_1][1,4,7,24,27,30,14,17,37,40]-hexaoxatetraazacyclohexatetracontin-51,52,53,54-tetrolato-(4-)-N^5,N^{50},O^{51},O^{54}:$N^{25},N^{30},O^{52},O^{53}$:$O^{12},O^{15},O^{18},O^{37},O^{40},O^{43},O^{51},O^{52},O^{53},O^{54}$]bis(copper)]cesium(1+) trifluoromethanesulfonate (10d): green solid; yield 57%, mp 255 °C dec (MeOH, and DIP as precipitant); IR (KBr) 1608 (N=C) cm^{-1}; FAB mass spectrum, m/e 1094 [(M - CF_3SO_3 + H)$^+$, calcd 1094]. Anal. Calcd for $C_{49}H_{40}CsCu_2F_3N_4O_{13}S\cdot 3H_2O$: Cs, 10.2; Cu, 10.2. Found: Cs, 10.1; Cu, 10.8. Karl–Fisher titration calcd for $3.0H_2O$: H_2O, 4.30. Found: H_2O, 4.30.

[μ_3-[13,14,16,17,38,39,41,42-Octahydro-7,11:19,23:32,36:44,48-tetramethenodibenzo[o,l_1][1,4,7,24,27,30,14,17,37,40]-hexaoxatetraazacyclohexatetracontin-51,52,53,54-tetrolato-(4-)-N^5,N^{50},O^{51},O^{54}:$N^{25},N^{30},O^{52},O^{53}$:$O^{12},O^{15},O^{18},O^{37},O^{40},O^{43},O^{51},O^{52},O^{53},O^{54}$]bis(nickel)]cesium(1+) trifluoromethanesulfonate (10e): brown solid; yield 40%; mp 275 °C dec; ^{1}H NMR (DMSO-d_6) δ 7.95 (s, 4 H, N=CH), 7.8–7.6 (m, 4 H, Ar' H), 7.5–7.3 (m, 4 H, Ar' H), 6.9–6.7 (m, 4 H, Ar H), 6.6–6.3 (m, 8 H, Ar H), 4.1–3.7 (m, 16 H, OCH_2); IR (KBr) 1610 (N=C) cm^{-1}; FAB mass spectrum, m/e 1082 [(M - CF_3SO_3)$^+$, calcd 1082]. Anal. Calcd for $C_{49}H_{40}CsF_3N_4Ni_2O_{13}S\cdot 2.8H_2O$: C, 46.08; H, 3.38; Cs, 10.3; N, 4.39. Found: C, 45.72; H, 3.59; Cs, 10.4; N, 4.36. Karl–Fisher titration calcd for $2.8H_2O$: H_2O, 3.93. Found: H_2O, 3.97.

[μ_3-[13,14,16,17,38,39,41,42-Octahydro-7,11:19,23:32,36:44,48-tetramethenodibenzo[o,l_1][1,4,7,24,27,30,14,17,37,40]-hexaoxatetraazacyclohexatetracontin-51,52,53,54-tetrolato-(4-)-N^5,N^{50},O^{51},O^{54}:$N^{25},N^{30},O^{52},O^{53}$:$O^{12},O^{15},O^{18},O^{37},O^{40},O^{43},O^{51},O^{52},O^{53},O^{54}$]bis(zinc)]cesium(1+) trifluoromethanesulfonate (10f): yellow solid; yield 64%; mp >300 °C; ^{1}H NMR (DMSO-d_6) δ 8.99 (s, 4 H, N=CH), 8.0–7.6 (m, 4 H, Ar' H), 7.5–7.2 (m, 4 H, Ar' H), 7.1–6.7 (m, 4 H, Ar H), 6.6–6.2 (m, 8 H, Ar H), 4.3–3.8 (m, 16 H, OCH_2); IR (KBr) 1614 (N=C) cm^{-1}; FAB mass spectrum, m/e 1096 [(M - CF_3SO_3)$^+$, calcd 1096]. Anal. Calcd for $C_{49}H_{40}CsF_3N_4O_{13}SZn_2\cdot 4H_2O$: C, 44.66; H, 3.67; N, 4.25. Found: C, 44.84; H, 3.55; N, 4.25. Karl–Fisher titration calcd for $4H_2O$: H_2O, 5.47. Found: H_2O, 5.40.

[μ_3-[13,14,16,17,38,39,41,42-Octahydro-7,11:19,23:32,36:44,48-tetramethenodibenzo[o,l_1][1,7,24,30,4,27,14,17,37,40]-tetraoxadithiatetraazacyclohexatetracontin-51,52,53,54-tetrolato(4-)-N^5,N^{50},O^{51},O^{54}:$N^{25},N^{30},O^{52},O^{53}$:$O^{12},O^{18},O^{37},O^{43},O^{51},O^{52},O^{53},O^{54},S^{15},S^{40}$]bis(copper)]barium(2+) bis(trifluoromethanesulfonate) (10g): green solid; yield 67%; mp >300 °C (MeOH, and DIP as precipitant); IR (KBr) 1608 (N=C) cm^{-1}; FAB mass spectrum, m/e 1279 [(M - CF_3SO_3)$^+$, calcd 1279]. Anal. Calcd for $C_{50}H_{40}BaCu_2F_6N_4O_{14}S_4\cdot H_2O$: C, 41.54; H, 2.93; N, 3.88. Found: C, 41.33; H, 2.78; N, 3.73.

[μ_3-[13,14,16,17,38,39,41,42-Octahydro-7,11:19,23:32,36:44,48-tetramethenodibenzo[o,l_1][1,7,24,30,4,27,14,17,37,40]-tetraoxadithiatetraazacyclohexatetracontin-51,52,53,54-tetrolato(4-)-N^5,N^{50},O^{51},O^{54}:$N^{25},N^{30},O^{52},O^{53}$:$O^{12},O^{18},O^{37},O^{43},O^{51},O^{52},O^{53},O^{54},S^{15},S^{40}$]bis(nickel)]barium(2+) bis(trifluoromethanesulfonate) (10h): brown solid; yield 74%; mp 280 °C dec; ^{1}H NMR (DMSO-d_6) δ 8.47 (s, 4 H, N=CH), 7.8–7.6 (m, 4 H, Ar' H), 7.6–7.2 (m, 4 H, Ar' H), 7.1–6.8 (m, 4 H, Ar H), 6.8–6.4 (m, 8 H, Ar H), 4.3–3.9 (m, 8 H, OCH_2), 3.2–2.9 (m, 8 H, SCH_2); IR (KBr) 1609 (N=C) cm^{-1}; FAB mass spectrum, m/e 1267 [(M - CF_3SO_3)$^+$, calcd 1267]. Anal. Calcd for $C_{50}H_{40}BaF_6N_4Ni_2O_{14}S_4\cdot 3H_2O$: C, 40.80; H, 3.15; N, 3.81. Found: C, 40.77; H, 2.96; N, 3.72.

X-ray Crystallography. X-ray diffraction measurements were performed on a Philips PW1100 or an Enraf-Nonius CAD4 diffractometer, using graphite-monochromated Mo Kα (λ = 0.71073 Å) radiation. Crystal data and data collection parameters are collected in Table II. Lattice parameters were determined by least squares from 25 centered reflections. Intensities were measured in the $\omega/2\theta$ scan mode and are corrected for decay of three control reflections, measured every hour, and for Lorentz and polarization factors. The complete data of the crystallographic studies of the compounds **9b** and **10a**·$2H_2O$ have been deposited at the Cambridge Crystallographic Data Base.[1]

The metal ions were located by Patterson methods and the rest of the heavy atoms by successive difference Fourier syntheses. Reflections with $F_o^2 > 5\sigma(F_o^2)$ for **9b** and **10a** and $F_o^2 > 3\sigma(F_o^2)$ for **10b** were considered observed and were included in the refinement (on F) by full-matrix least squares. Weights were calculated as $w = 4F_o^2/\sigma^2(F_o^2)$, with $\sigma^2(F_o^2) = \sigma^2(I) + (pF_o^2)^2$, $\sigma(I)$ being based on counting statistics and p being an instability factor obtained from plots of F_o vs weighted error. In all structures the metal ions were refined with anisotropic thermal parameters, and depending on the ratio of data:parameters and the presence of disorder, other atoms were also refined anisotropically. Noncoordinated triflate anions were often disordered. For all the three structures an empirical absorption correction, using DIFABS,[32] was performed. No hydrogens were included for **9b**, and for **10a** and **10b** the hydrogens were put in calculated positions and they were treated as riding on their parent carbon atoms. Parameters refined were the overall scale factor, the isotropic extinction parameter g [$F_{corr} = F_c/(1 + gI_c)$], if included, positional and isotropic or anisotropic thermal parameters. Final difference Fourier maps showed no significant features. All calculations were done by using SDP.[33]

Electrochemistry. The sampled DC polarography and Kalousek measurements were carried out with a Metrohm E505 polarograph. This polarograph was operated in a three-electrode mode with a dropping mercury electrode (DME) as working electrode, a platinum wire as auxiliary electrode and an Ag/AgCl electrode (Metrohm EA 441/5) as reference. The reference electrode was filled with 1 M $Et_4N^+Cl^-$ (Merck, synthetic quality, recrystallized from ethyl acetate/$CHCl_3$) in MeOH (Merck, pa quality). The measurements were performed at 20 °C in a 0.1 M solution of TEAP ($Et_4N^+ClO_4^-$, Fluka, purum, recrystallized from EtOH) in DMSO (pa quality of Merck, max 0.03% H_2O). The reference electrode was brought into contact with the sample via a double salt bridge of the following configuration:

Ag; AgCl, $Et_4N^+Cl^-$–MeOH:TEAP–DMSO:sample

The characteristics of the DME electrode were: m = 1.065 mg/s, natural drop time = 5.30 s, and height of the mercury column = 64 cm. A mechanical drop time of 1.000 s was maintained during all experiments. Oxygen was expelled by bubbling with nitrogen (Hoekloos, very pure) for at least 10 min. DC_T polarograms were recorded and evaluated by a computerized method described by Zollinger et al.[24] A reference compound was measured several times during the day to detect fluctuations ($\Delta E_{1/2} < 3$ mV).

Cyclic voltammetry was carried out with an AUTOLAB computerized system for electrochemistry (ECO CHEMIE, Utrecht, The Netherlands). The measurements were performed at a stationary hanging mercury drop electrode (Metrohm, 663 VA Stand). The same reference and auxiliary electrode were used as in the polarographic experiments. The solvent and the supporting electrolyte were also the same as used in the polarography.

Coulometry was carried out with a Metrohm Coulostat E524 and a Metrohm Integrator E525. A recorder was connected to the integrator to record the current–time curve. The measurements were carried out in the same solvent and supporting electrolyte as were used for the polarographic experiments. An H-type of cell was used. One compartment contained a mercury pool as working electrode and a reference electrode and the other compartment a platinum counter electrode. The two compartments were connected by a salt bridge. The reference electrode was the same as used for the other electrochemical experiments. The coulostat was operated with a constant potential (potentiostatic coulometry).

(32) Walker, N.; Stuart, D. *Acta Crystallogr., Sect. A* **1983**, *39*, 158.
(33) *Structure Determination Package*; B. A. Frenz and Associates Inc.: College Station, TX, and Enraf-Nonius: Delft, 1983.

EPR Spectroscopy. EPR spectra of powdered samples in frozen solutions (about 0.01 M in MeOH at 77 K) were recorded on a Varian E3 instrument. Field calibrations were done using DPPH. EPR spectra with varying amounts of exogenous ligands were performed by controlled addition of Bu_4NF and NaIm (Im = imidazolate) to the EPR solution before rapid cooling to 77 K, and warming up after each spectrum.

Acknowledgment. We thank Akzo International research BV for financial support and Mr. F. B. Hulsbergen (Leiden University, Department of Chemistry) for recording the EPR spectra. Of the Department of Chemical Analysis (University of Twente) we thank J. M. Visser and J. L. M. Vrielink for recording the ^1H and ^{13}C NMR spectra and IR spectra, T. Stevens for recording the mass spectra, and A. Montanaro-Christenhusz and H. Weber for the elemental analyses.

Registry No. 1, 24677-78-9; 2, 7460-82-4; 3a, 121073-78-7; 3b, 130642-27-2; 4, 108059-04-7; 5, 130642-25-0; 6, 130642-26-1; 7, 130668-80-3; 8, 95-54-5; 9b, 121073-80-1; 9c, 130669-02-2; 9e, 130669-00-0; 10a, 121073-84-5; 10a·2H_2O, 130668-86-9; 10b, 121073-82-3; 10b·(H_2O, DMSO), 130668-83-6; 10c, 130668-98-3; 10d, 130668-96-1; 10e, 130668-94-9; 10f, 130668-92-7; 10h, 130668-90-5; 10i, 130668-88-1; $BrCH_2CH_2Br$, 106-93-4; $HOCH_2CH_2OH$, 107-21-1.

Supplementary Material Available: Tables of positional and thermal parameters of all atoms, bond distances, and bond angles in the dinickel/barium complex 10b·(H_2O,DMSO) (8 pages). Ordering information is given on any current masthead page.

Mechanistic Investigations Aided by Isotopic Labeling. 10.[1] Investigations of Novel Furan-2,3-dione Rearrangements by Oxygen-17 Labeling[2]

Gert Kollenz,* Heinz Sterk, and Gerald Hutter

Institute of Organic Chemistry, Isotope Department and Spectroscopic Department, Karl Franzens University Graz, Heinrichstrasse 28, A-8010 Graz, Austria

Received February 27, 1990

The oxa 1,3-diene moiety in 4-benzoyl-5-phenylfuran-2,3-dione (1) adds aryl isocyanides or heterocumulenes via formal [4 + 1] or [4 + 2] cycloaddition processes. The unstable primary adducts undergo novel furandione rearrangements to intermediates in which the two oxygen atoms of the lactone moiety in 1 are equivalent. This equivalence was confirmed by ^{17}O-labeling experiments using ^{17}O NMR spectroscopic and mass spectroscopic measurements. Comparison of the ^{17}O chemical shifts in 1, labeled either at the benzoyl and ring oxygens (1a-^{17}O) or at both exocyclic ring-carbonyl oxygens (1b-^{17}O), with those in the products 2-4 confirmed the proposed pathways of these rearrangements. Reactions involving carbodiimides, isocyanates, and ketene imines were investigated.

The addition of aryl isocyanides[3] or heterocumulenes[4] to the oxa diene moiety in 4-benzoyl-5-phenylfuran-2,3-dione (1) has been reported to afford various mono- and bicyclic heterocyclic systems. Their molecular skeletons were elucidated by single-crystal X-ray diffraction analyses and ^{13}C NMR measurements.[3,4] All the reaction pathways obviously include formal [4 + 1] or [4 + 2] cycloaddition processes (intermediate A, Scheme I) accompanied by novel furandione rearrangements. The latter should proceed via ring opening of the furan ring with formation of an oxo carboxylic side chain (B or C), which undergoes free rotation around the single bond to give heterocyclic systems by relactonization at the former benzoyl carbon. The net result is the exchange of the two phenyl groups in 1. Ring opening could be initiated by attack of the heterocumulene on the heterodiene system in 1, leading to intermediate E by a cycloreversion process (reaction pathway A → C → D → E). This cycloreversion could be effected either by the re-formation of the furandione ring or through intermediate D. Alternatively, fragmentation of the primary adduct A would lead to E via intermediate B

Scheme I

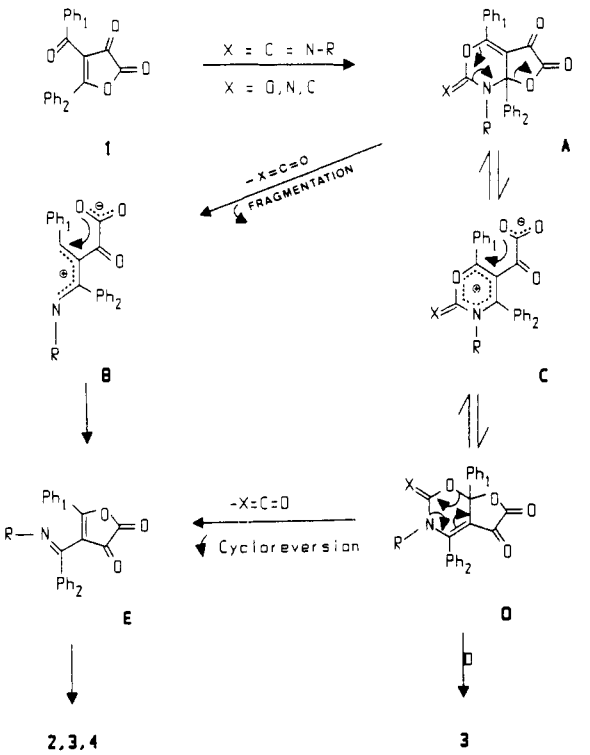

(reaction pathway A → B → E). In both reaction pathways the lactone oxygens in 1 become equivalent by free rotation in the ring-opened intermediates B or C, irrespective of

(1) For part 9, see: Kollenz, G.; Seidler, P. *Monatsh. Chem.* 1984, *115*, 623.

(2) Presented, in part, at the 2nd International Symposium on Synthetic Applications of Isotopically Labeled Compounds, Kansas City, 1985.

(3) Kollenz, G.; Ott, W.; Ziegler, E.; Peters, E.-M.; Peters, K.; von Schnering, H. G.; Formacek, V.; Quast, H. *Justus Liebigs Ann. Chem.* 1984, 1137.

(4) (a) Kollenz, G.; Penn, G.; Dolenz, G.; Akcamur, Y.; Peters, K.; Peters, E.-M.; von Schnering, H. G. *Chem. Ber.* 1984, *117*, 1299. (b) Kollenz, G.; Penn, G.; Ott, W.; Peters, K.; Peters, E.-M.; von Schnering, H. G. *Chem. Ber.* 1984, *117*, 1310. (c) Kollenz, G.; Penn, G.; Ott, W.; Peters, K.; Peters, E.-M.; von Schnering, H. G. *Heterocycles* 1987, *26*, 625.

0022-3263/91/1956-0235$02.50/0